MOLECULAR AND CELLULAR BIOLOGY, July 2001, p. 4097–4109 Vol. 21, No. 13
0270-7306/01/$04.00+0 DOI: 10.1128/MCB.21.13.4097–4109.2001


# Eukaryotic Initiation Factor 4G-Poly(A) Binding Protein Interaction Is Required for Poly(A) Tail-Mediated Stimulation of Picornavirus Internal Ribosome Entry Segment-Driven Translation but Not for X-Mediated Stimulation of Hepatitis C Virus Translation

YANNE M. MICHEL, ANDREW M. BORMAN, SYLVIE PAULOUS, AND KATHERINE M. KEAN*

*U.P. Régulation de la Traduction Eucaryote et Virale, CNRS URA 1966, Institut Pasteur, 75724 Paris Cedex 15, France*

Received 8 November 2000/Returned for modification 20 December 2000/Accepted 4 April 2001

**Efficient translation of most eukaryotic mRNAs results from synergistic cooperation between the 5′ $m^7$GpppN cap and the 3′ poly(A) tail. In contrast to such mRNAs, the polyadenylated genomic RNAs of picornaviruses are not capped, and translation is initiated internally, driven by an extensive sequence termed IRES (for internal ribosome entry segment). Here we have used our recently described poly(A)-dependent rabbit reticulocyte lysate cell-free translation system to study the role of mRNA polyadenylation in IRES-driven translation. Polyadenylation significantly stimulated translation driven by representatives of each of the three types of picornaviral IRES (poliovirus, encephalomyocarditis virus, and hepatitis A virus, respectively). This did not result from a poly(A)-dependent alteration of mRNA stability in our in vitro translation system but was very sensitive to salt concentration. Disruption of the eukaryotic initiation factor 4G-poly(A) binding protein (eIF4G-PABP) interaction or cleavage of eIF4G abolished or severely reduced poly(A) tail-mediated stimulation of picornavirus IRES-driven translation. In contrast, translation driven by the flaviviral hepatitis C virus (HCV) IRES was not stimulated by polyadenylation but rather by the authentic viral RNA 3′ end: the highly structured X region. X region-mediated stimulation of HCV IRES activity was not affected by disruption of the eIF4G-PABP interaction. These data demonstrate that the protein-protein interactions required for synergistic cooperativity on capped and polyadenylated cellular mRNAs mediate 3′-end stimulation of picornaviral IRES activity but not HCV IRES activity. Their implications for the picornavirus infectious cycle and for the increasing number of identified cellular IRES-carrying mRNAs are discussed.**

The initiation of protein synthesis on most mRNAs in eukaryotes follows binding of the 40S ribosomal subunit near the capped 5′ end of the mRNA and subsequent migration of this subunit along the mRNA in a 5′-to-3′ direction until a suitable initiation codon is selected (for a review, see reference 29). Recognition of the mRNA 5′ end and 40S subunit recruitment requires the eukaryotic initiation factor (eIF) 4F complex (for reviews, see references 35 and 43). The eIF4F complex comprises the cap binding protein (eIF4E) and an ATP-dependent RNA helicase (eIF4A) bound, respectively, toward the N and C termini of a scaffold protein, eIF4G (for a review, see references 14 and 35). The C-terminal half of eIF4G is also thought to associate with the multisubunit eIF3 complex, which binds the 40S ribosomal subunit directly thus bridging the gap between the mRNA 5′ end and the 40S subunit (reviewed in reference 17).

The vast majority of eukaryotic mRNAs are not only capped at their 5′ end but are also polyadenylated at their 3′ end. Aside from a role in mRNA metabolism (see reference 45 for a review), the poly(A) tail functions as a translational enhancer and interacts synergistically with the 5′ cap to stimulate translation initiation (12, 23, 42, 43). This cooperativity between the cap and poly(A) requires the poly(A) binding protein (PABP) (48). PABP has been shown to bind the N-terminal part of eIF4G in mammals (19, 41), plants (31), and yeast (49), leading to the suggestion that efficiently translated mRNAs are circularized via a cap-eIF4E-eIF4G-PABP-poly(A) tail interaction (the closed-loop model [23]). Indeed, capped and polyadenylated mRNAs can be circularized in vitro using purified yeast eIF4E, eIF4G, and PABP (51). Moreover, at least in mammalian systems, the integrity of the eIF4G-PABP interaction is critical for cap-poly(A) cooperativity (34), and this interaction results in an increased functional affinity of eIF4E for the capped mRNA 5′ end (8).

The animal picornaviruses bear witness to an alternative mode of translation initiation. Their uncapped, polyadenylated genomes which serve as mRNAs contain an extensive (ca. 450 nucleotides [nt]), heavily structured sequence within the 5′ noncoding region, known as the IRES (for internal ribosome entry segment). This allows direct internal entry of ribosomes some several hundred nucleotides from the RNA 5′ end (for a review, see reference 22). Thus, translation of the picornaviral RNAs is both cap and 5′-end independent. A similar mechanism of translation initiation has been described for the flavivirus, hepatitis C virus (HCV), whose uncapped and nonpolyadenylated, positive-strand RNA genome also carries an IRES (20, 38; for a review, see reference 22). In fact, IRESes have now been identified in many cellular mRNAs (for a review, see reference 9), and various lines of evidence suggest that up to or even more than 10% of cellular mRNAs may be translated by internal initiation. Hence, the question of how cap- and 5′-

* Corresponding author. Mailing address: U.P. Régulation de la Traduction Eucaryote et Virale, CNRS URA 1966, Institut Pasteur, 25 rue du Dr. Roux, 75724 Paris Cedex 15, France. Phone: (33) 1-40-61-33-55. Fax: (33) 1-40-61-30-45. E-mail: kathiemb@pasteur.fr.

end-independent translation can be encompassed in a closed-loop translation model is extremely pertinent.

In effect, it has been postulated that picornaviral RNAs and HCV RNA would be difficult to accommodate within the form of the closed-loop translation model proposed for classical cellular mRNAs (for a review, see reference 26). Aside from the different natures of the 3′ and/or 5′ ends of these viral mRNAs compared to the majority of cellular mRNAs, one must take into consideration the known factor requirements for viral IRES-driven translation initiation. Most picornavirus genomes encode proteinases which cleave components of the eIF4F complex. Thus, the entero-and rhinoviral 2A proteinases and the aphthoviral L proteinase cleave eIF4G (28, 32) to separate the N-terminal eIF4E- and PABP-binding domains from the C-terminal eIF3- and eIF4A-binding regions (30). Furthermore, the entero- and rhinovirus 3C and/or 2A proteinases were recently demonstrated to induce cleavage of PABP both in vitro and in the infected cell (25, 27; A. M. Borman, Y. M. Michel, and K. M. Kean submitted for publication). These cleavage events account, at least in part, for the dramatic shutoff of host cell translation observed during infection with all picornaviruses, except for hepatitis A virus (HAV). With the exception of the HAV IRES, which requires intact eIF4G for activity (5), picornaviral IRES-driven translation continues unabated upon eIF4G cleavage (2). Effectively, entero-, rhino-, cardio-, and aphthoviral IRES activity requires only the C-terminal cleavage product of eIF4G and its associated proteins, which do not include eIF4E or PABP (6, 33, 36). Indeed, the C-terminal cleavage product of eIF4G or a recombinant fragment spanning part of this cleavage product has been shown to interact directly with these IRESes (33, 39; Borman et al. submitted) and can substitute for intact eIF4G in 48S initiation complex formation on the encephalomyocarditis virus (EMCV) IRES (37). HCV represents an even more extreme case, since eIF4F is not needed at all for the binding of ribosomal subunits to this IRES (38).

Nevertheless, it seems clear that the efficiency of picornavirus IRES-driven translation is dependent on the nature of the 3′ end of the mRNA. Even though the poly(A) tails of picornaviral RNAs are heterogeneous in length, good evidence exists that poly(A)$^-$ picornavirus genomes have a considerably reduced infectivity (15, 44, 46). Although this reduction in infectivity may partly reflect a role of the poly(A) tail in viral RNA synthesis, it has long been known that translation of EMCV genomic RNA is moderately increased in vitro as the length of the poly(A) tail is increased (18). Using artificial reporter RNAs, we recently showed that translation from the EMCV IRES is indeed stimulated approximately threefold upon polyadenylation of the mRNA in appropriate in vitro systems (34). Furthermore, it has since been reported that such poly(A) tail-mediated stimulation of translation is also exhibited by the other two classes of picornaviral IRESes (1). Similarly, translation driven by the flaviviral HCV IRES is significantly increased on mRNAs which carry the authentic viral 3′ end (20), which in this case is not a poly(A) tail but a conserved three-stem-loop structure which binds polypyrimidine tract-binding protein (50).

To date, no study has been undertaken which attempts to address the underlying molecular mechanisms of 3′-end stimulation of IRES-driven translation, other than our reported results restricted to the EMCV IRES (34). In the light of the data outlined above, and of the role of the eIF4G-PABP interaction in synergistically stimulating capped and polyadenylated cellular mRNA translation, the aim of the current work was to evaluate the factors required for mRNA 3′-end-mediated stimulation of IRES-driven translation. Using our recently described poly(A)-dependent rabbit reticulocyte lysate extracts (34), we confirm that polyadenylation significantly stimulates translation driven by the picornaviral HAV, EMCV, and poliovirus (PV) IRESes but not that driven from the unrelated flaviviral HCV IRES.

Of more novel import, we show that poly(A)-mediated stimulation of picornaviral IRES activity requires the integrity of the eIF4G-PABP interaction, indicating that mRNA 5′-3′ cross talk is mechanistically conserved between classical eukaryotic mRNAs and picornaviral IRES-carrying RNAs. Furthermore, we present data indicative of jettisoning of 5′ to 3′-end cross talk in the case of PV IRES-carrying RNAs upon shutoff of host cell translation. Finally, we show that the mechanism of HCV IRES translation stimulation mediated by the cognate viral 3′ end is distinct from that of classical eukaryotic mRNAs.

## MATERIALS AND METHODS

**Plasmid constructions and in vitro transcriptions.** The plasmids used in this work are represented schematically in Fig. 1. Plasmids were derived from the previously described p0p24 (34), which contains, under the control of the T7 promoter, a short oligonucleotide-derived 5′ untranslated region (UTR), followed by the region coding for the human immunodeficiency virus (HIV-$1_{Lai}$) p24 protein and the influenza virus NS 3′ UTR. Two versions of this plasmid differ only in the presence or absence of an $A_{50}$ tract inserted at the unique *Eco*RI site, located 24 nt downstream of the authentic polyadenylation signal.

All IRES-containing constructs were obtained by inserting the region corresponding to each entire IRES into the poly(A)$^+$ and poly(A)$^-$ forms of p0p24. pPVp24 was obtained by inserting the PV IRES, namely, the in-filled *Asp*718-*Msc*I fragment (nt 67 to 630) from pKK-C2 (3), into the in-filled *Sal*I site of p0p24. pEMCVp24 was constructed by inserting the EMCV IRES (from the polyC tract to nt 848, i.e., the in-filled *Eco*RI-*Nco*I small fragment from p-CITE; Novagen) into the in-filled *Bam*HI site of p0p24. pHAVp24 resulted from the insertion of the in-filled *Nco*I-*Afl*II fragment (nt 44 to 738) of the full-length cDNA clone of HAV (p16HM175 [24]) into the in-filled *Bam*HI site of p0p24. pHCVp24 was generated by inserting the *Sal*I-*Bam*HI short fragment from the bicistronic pXLJ-HCV construct (2), which includes nt 40 to 372 of the HCV genome, into p0p24 which had been digested with the same enzymes. Thus, each plasmid was constructed in such a way that the minimal sequences required for efficient IRES activity were maintained.

Plasmids containing the 3′ UTR X region from the HCV were derived from the poly(A)$^-$ p0p24 or pHCVp24 plasmids by inserting annealed 5′-AATTGG TGGCTCCATCTTAGCCCTAGTCACGGCTAGCTGTGAAAGGTCCGTG AGCCGCATGACTGCAGAGAGTGCTGATACTGGCCTCTCTGCAGTCA TGTG-3′ and 5′-AATTCACATGACTGCAGAGAGGCCAGTATCAGCACT CTCTGCAGTCATGCGGCTCACGGACCTTTCACAGCTAGCCGTGACT AGGGCTAAGATGGAGCCACC-3′ oligonucleotides into the unique *Eco*RI site at the 3′ end of the NS 3′ UTR. All constructs were verified by sequencing.

In vitro transcriptions, performed on plasmids linearised by *Eco*RI, and quantification and purification of the synthesized transcripts were done exactly as described previously (34).

**Antibodies and recombinant proteins.** Rabbit anti-eIF4G peptide 7 antiserum (raised against residues 327 to 342) and monoclonal antibody 10E10 raised against human PABP have been described previously (16, 52). Recombinant wild-type human rhinovirus 2A proteinase, expressed in *Escherichia coli* and purified to homogeneity as described previously (32) was a gift from T. Skern. A recombinant fragment of rotavirus NSP3 protein encompassing amino acids 163 to 313, overexpressed in *E. coli* and purified exactly as described previously (40, 41), was a gift from D. Poncet. Both 2A proteinase and NSP3 were dialyzed against H100 buffer (10 mM HEPES-KOH, pH 7.5; 100 mM KCl; 1 mM $MgCl_2$; 0.1 mM EDTA; 7 mM β-mercaptoethanol) prior to use.

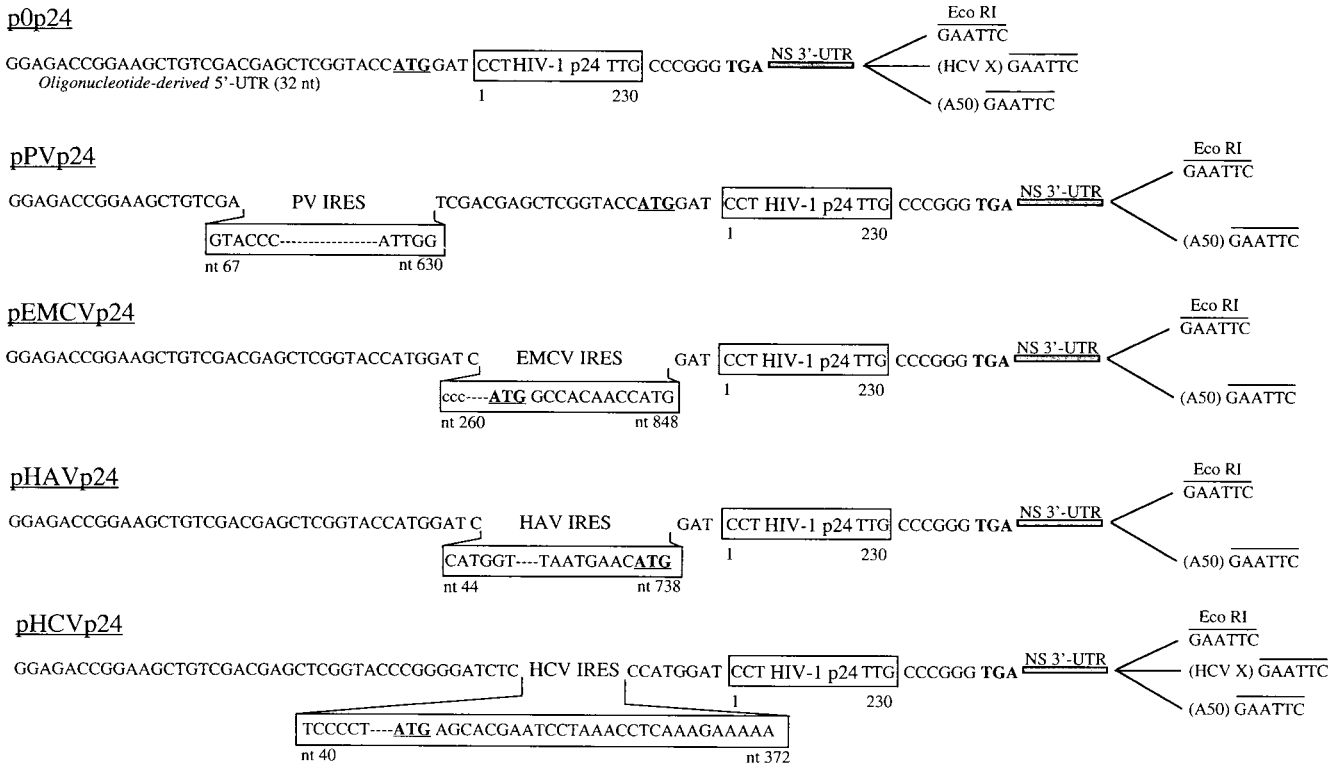


FIG. 1. Schematic representation of the plasmids used in this work. The HIV-1p24 coding region and the regions corresponding to the different IRESes are shown as open boxes. Numbers below the coding region refer to the first and last amino acids of HIV-1p24, and numbering below the IRESes denotes the first and last nucleotides of the corresponding viral genome sequences. The ATG codon initiating HIV-1p24 synthesis is shown in boldface and is underlined; the TGA stop codon is shown in boldface. The NS 3′ UTR is depicted as a thick speckled line. Clones were constructed either in duplicate, differing only by the presence or absence of an $A_{50}$ insertion (bracketed) at the *Eco*RI site used for linearization prior to transcription, or in triplicate (p0p24 and pHCVp24) including, instead of the $A_{50}$ oligonucleotide, 98 nt corresponding to the 3′ X region from the HCV genome (bracketed).

**Preparation of translation extracts and in vitro translations.** Nuclease-treated Flexi-rabbit reticulocyte lysates (Promega) were partially depleted of ribosomes by ultracentrifugation in a Beckman TL-100 benchtop ultracentrifuge as described previously (8, 34). Translation reactions (12 μl, final volume) containing 50% by volume RRL or ribosome-depleted RRL and 33% by volume H100 buffer were programmed with the indicated concentrations of in vitro-transcribed mRNAs. For pPVp24-derived mRNAs, reactions contained HeLa cell S10 extract (to 2.5% [vol/vol]) prepared as described earlier (3). Reactions which included recombinant proteins were preincubated with the indicated concentrations of 2A proteinase or NSP3 (each diluted in H100 buffer) for 10 min at 30°C (for 2A) or 4°C (for NSP3) before the addition of RNA. The final concentrations of added KCl and $MgCl_2$ in translation reactions were 130 and 0.9 mM, respectively, for p0p24 and were varied according to the IRES-containing mRNAs used as indicated. Translations were performed at 30°C (typically for 90 min) in the presence of [$^{35}$S]methionine. In certain experiments, RNAs labeled with trace quantities of $^{32}$P were extracted from translation reactions prior to retranslation in fresh extracts. Briefly, at the appropriate times, translation reactions were placed on ice and made 5 mM in EDTA. After 5 min at 4°C, reactions received 10 volumes of extraction buffer (200 mM NaCl; 10 mM Tris-HCl, pH 9; 1 mM EDTA; 1% sodium dodecyl sulfate [SDS]) and were extracted twice with phenol and chloroform. Nonaqueous phases were back extracted with extraction buffer, extracted RNA was precipitated by ethanol, and the RNA pellet was washed with 70% ethanol. Extracted RNA was quantified by scintillation counting prior to retranslation.

Translation products were analyzed by SDS-polyacrylamide gel electrophoresis as described previously (11), using gels containing 20% (wt/vol) polyacrylamide. Dried gels were exposed to Bio-max MR film (Kodak) for 1 to 15 days, depending on the experiments. Densitometric quantification of translation products was performed exactly as described previously (5), using multiple exposures of each gel to ensure that the linear response range of the film was respected. The data presented in each figure are representative of at least three independent translation assays.

**Western blotting analysis.** Western blot analysis of eIF4G or PABP was performed exactly as described previously (6) using rabbit anti-eIF4G peptide 7 antisera (for detection of the N-terminal cleavage product of eIF4G) or monoclonal antibody 10E10 (for PABP) as primary antibodies. Membranes were then incubated with horseradish peroxidase-linked goat anti-mouse or anti-rabbit secondary antibodies and were revealed by enhanced chemiluminescence (ECLplus; Amersham) or the commercial DAB peroxidase substrate kit (Vector Laboratories, Inc.).

## RESULTS

Efficient translation of classical cellular mRNAs requires cooperative interplay between the 5′ cap structure and 3′ poly(A) tail [cap-poly(A) synergy (12, 23, 42, 48)]. We recently described a nuclease-treated, ribosome-depleted rabbit reticulocyte lysate (RRL) cell-free translation system which recapitulates cap-poly(A) synergistic stimulation of cellular mRNA translation in vitro (34). Polyadenylation stimulated translation driven by the one IRES tested in this system, that of the picornavirus EMCV (34). Thus, the aims of the current study were to confirm that polyadenylation stimulates translation driven by all picornaviral IRESes in our ribosome-depleted RRL system and, more importantly, to investigate the molecular mechanisms involved. The flaviviral HCV IRES was also

studied, since this viral RNA is nonpolyadenylated and the viral 3′ X region has previously been reported to stimulate HCV IRES activity in vitro (20). Toward this end, different cDNAs were constructed which could be used to generate monocistronic mRNAs in which representatives of the three major classes of picornaviral IRESes precede an identical reporter gene (HIV-1 p24) and 3′-UTR (Fig. 1). Two different cDNA templates were generated for each IRES, which differed only by the presence or absence of an $A_{50}$ tract inserted at the restriction site used for linearization prior to in vitro transcription. A series of similar cDNAs was also constructed to carry the HCV IRES but including a construction with the viral 3′ X region, which has previously been reported to stimulate HCV IRES activity in vitro (20).

While the type II cardio- and aphthoviral IRESes and the type III HAV IRES are functional in an unadulterated RRL system, the type I entero- and rhinoviral IRESes are virtually inactive in RRL which has not been supplemented with cytoplasmic extracts from permissive cells such as HeLa cells (2, 4). Thus, we first verified that a ribosome-depleted RRL supplemented with a nucleased HeLa cell S10 extract still exhibited cap-poly(A) cooperative stimulation of cellular mRNA translation. Translation of monocistronic p0p24-derived cellular mRNAs in standard RRL is strongly stimulated by capping and modestly stimulated by polyadenylation, and the combined effects of cap and poly(A) are at best additive (Fig. 2, RRL lanes [34]). However, when the same RNAs are translated in ribosome-depleted RRL, the stimulation observed upon capping and polyadenylation of an mRNA is much greater than the sum of the effects of cap and poly(A) alone (Fig. 2, ribosome-depleted RRL + H100 lanes, cap-poly(A) synergy of 4.5-fold). Importantly, cap-poly(A) synergy, although quantitatively reduced, is still observed in ribosome-depleted RRL supplemented with low concentrations of nuclease-treated HeLa cell S10 extract (Fig. 2, ribosome-depleted RRL + 2.5% S10 lanes), indicating that the potential effects of polyadenylation on entero- and rhinoviral IRES-driven translation can be examined in this system.

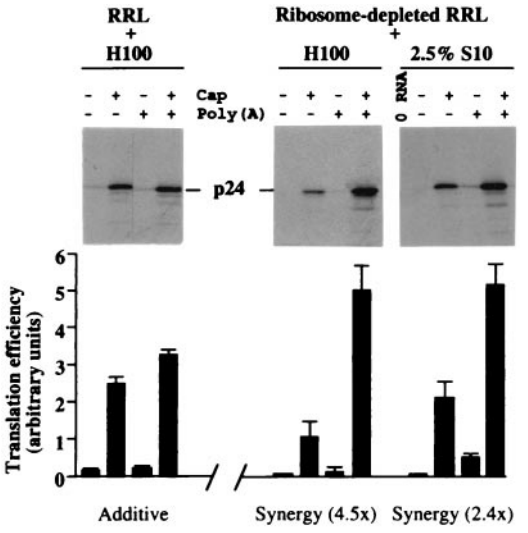


FIG. 2. Cap-poly(A) synergistic stimulation of cellular mRNA translation in ribosome-depleted RRL. Translation reactions containing standard RRL or ribosome-depleted RRL (see Materials and Methods) were programmed with 6.3 μg of p0p24 derived mRNAs per ml transcribed in the form indicated above each lane and contained 33% by volume of H100 buffer or 30.5% H100 and 2.5% nuclease-treated HeLa cell S10 extract in H100 buffer as indicated. A control reaction was programmed with water (0 RNA lane). The autoradiograph of the dried 20% polyacrylamide gel is shown. The position of the p24 protein is indicated. The translation efficiency was determined densitometrically as described in Materials and Methods and is plotted below each lane (in arbitrary units). Cap-poly(A) synergy is indicated below the panel where appropriate and was calculated according to the following formula: stimulation upon capping and polyadenylation/(stimulation upon capping + stimulation upon polyadenylation). The autoradiographs of reactions performed in ribosome-depleted RRL were exposed 12 times longer than those performed in standard RRL; hence, the broken *x* axis in the histogram. The error bars represent the standard deviation calculated from at least two independent experiments.

**The poly(A) tail stimulates translation driven by picornaviral, but not a flaviviral, IRESes in ribosome-depleted RRL.** Picornaviral RNAs are naturally uncapped. Thus, to examine the possible role of poly(A) in IRES-driven translation initiation, only two different forms of the various IRES-p24 monocistronic mRNAs, which carry or lack a 3′-terminal homopolymer $A_{50}$ tail, were generated in vitro (see Fig. 1 and Materials and Methods). These different mRNAs were then translated in ribosome-depleted RRL (for the type II EMCV and type III HAV IRESes and the flaviviral HCV IRES) or in ribosome-depleted RRL containing 2.5% by volume of nucleased HeLa cell S10 extract (for the type I PV IRES). This concentration of S10 extract had previously been determined to be the minimal supplement necessary to activate the PV IRES in depleted RRL (data not shown). Given that cap-poly(A) synergy on classical mRNAs in the depleted system is extremely sensitive to the concentrations of added KCl and $MgCl_2$ (8), the various polyadenylated and nonpolyadenylated IRES-containing mRNAs were translated at a range of final salt concentrations (Fig. 3).

The three different picornavirus IRESes exhibited significantly different KCl and $MgCl_2$ optima for translation, as has previously been reported in the standard RRL system (2). More interestingly, translation driven by the PV, HAV, and EMCV IRESes was reproducibly stimulated upon polyadenylation in a salt-sensitive manner. The greatest poly(A)-mediated stimulation was observed with the HAV IRES, which also exhibited the lowest KCl and $MgCl_2$ optima for translation (Fig. 3C). As the concentration of either KCl or $MgCl_2$ was increased, the magnitude of the poly(A) effect on the HAV IRES significantly increased, from ca. 3-fold at the lowest KCl and $MgCl_2$ concentrations tested to exceed 10-fold at the highest salt concentrations in which translation activity could be easily measured (14-fold stimulation at 108 mM added KCl; 12-fold stimulation at 0.9 mM added $MgCl_2$; Fig. 3C). The salt optima for PV IRES-driven translation were significantly higher than those of the HAV IRES. Poly(A)-mediated stimulation of PV IRES activity increased significantly as the KCl and $MgCl_2$ concentrations were increased, in a similar manner to that observed with the HAV IRES, but was reproducibly quantitatively lower than for the HAV counterpart (ca. sevenfold stimulation with 115 to 120 mM KCl and fourfold stimulation with 1.1 mM $MgCl_2$; Fig. 3A). It remains to be determined whether this reflects a real reduction in poly(A) dependency of the PV IRES compared to its HAV counterpart

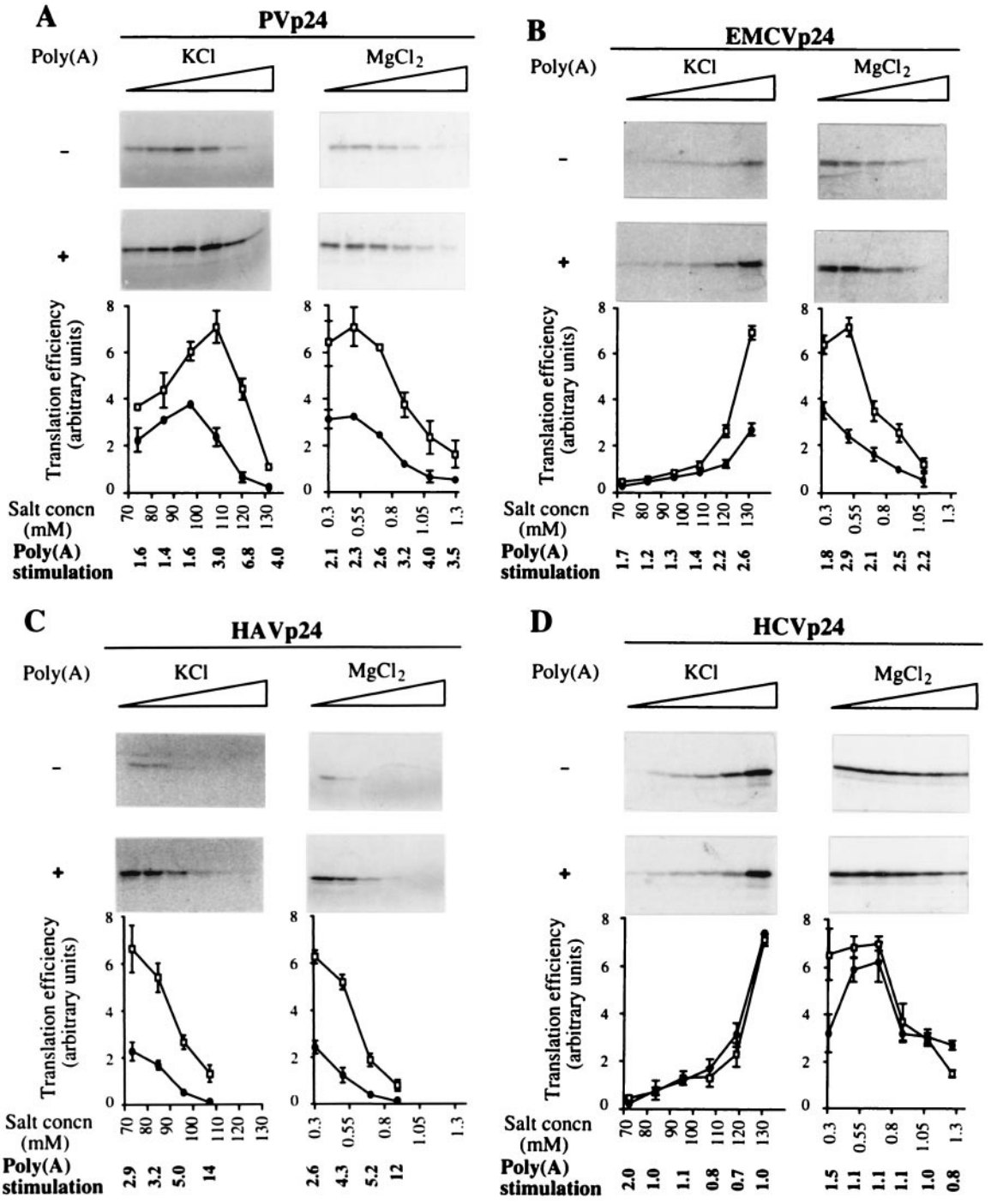


FIG. 3. Effects of polyadenylation on IRES-driven translation initiation in ribosome-depleted RRL. Ribosome-depleted RRL was programmed with poly(A)$^-$ or poly(A)$^+$ uncapped IRES-containing mRNAs (final concentration, 10 μg/ml). Translation reactions contained 0.9 mM added $MgCl_2$ (or 0.5 mM for HAVp24) and various concentrations of added KCl (from 72 to 130 mM; left panels) or 130 mM (EMCVp24 and HCVp24), 119 mM (PVp24), or 72 mM (HAVp24) added KCl and varyious concentrations of added $MgCl_2$ (0.3 to 1.3 mM; right panels). Reactions programmed with PVp24 contained 2.5% (vol/vol) nuclease-treated HeLa cell S10 extract. Translation products were analyzed as described in the legend to Fig. 2. Translation efficiencies of the different RNAs [filled circles for poly(A)$^-$ and open squares for poly(A)$^+$ mRNAs] as a function of salt concentration were used to calculate the stimulations upon polyadenylation [ratio of poly(A)$^+$ to poly(A)$^-$ translation efficiency]. For EMCVp24 and HAVp24, the translation efficiencies are plotted, and poly(A) stimulation is calculated only for reactions where translation products were easily detectable. The error bars represent the standard deviation calculated from at least two independent experiments.

TABLE 1. Effects of polyadenylation on IRES-driven translation initiation in standard RRL

| Transcript | Added salt concn (mM)[a] | | Poly(A) stimulation[b] |
|---|---|---|---|
| | KCl | $MgCl_2$ | |
| PVp24[c] | 119 | 0.7 | 1.1 |
| EMCVp24 | 130 | 0.9 | 0.9 |
| HAVp24 | 72 | 0.5 | 1.7 |
| HCVp24 | 130 | 0.9 | 1.0 |

[a] Final concentrations in translation reactions.
[b] Calculated as the ratio of poly(A)$^+$/poly(A)$^-$ translation efficiencies (average of three different programming mRNA concentrations).
[c] Reactions contained 2.5% (vol/vol) nuclease-treated HeLa cell S10 extracts.

or rather stems from the inclusion of HeLa cell S10 extract in the depleted RRL reactions programmed with PVp24 RNAs. The EMCV IRES was also significantly stimulated by polyadenylation (stimulation of ca. two- to threefold; Fig. 3B), although in this case the stimulatory effect of poly(A) was relatively insensitive to altering the concentrations of $MgCl_2$. Thus, globally picornavirus IRES-driven translation was most stimulated by polyadenylation as the concentrations of KCl or $MgCl_2$ approached physiological levels. In addition, in a manner analogous to that reported recently for cap-poly(A) synergy in the ribosome-depleted RRL system, poly(A) stimulation was maximal at salt concentrations in excess of those optimal for translation driven by the PV or HAV IRESes. This apparent paradox reflects the fact that translation of nonpolyadenylated mRNAs carrying these IRESes was extremely inefficient in elevated concentrations of KCl or $MgCl_2$. Interestingly, the magnitude of the poly(A) effects on picornavirus IRES activity was not greatly affected by altering the concentrations of programming mRNA (data not shown), in contrast to cap-poly(A) synergy on cellular mRNAs in the depleted RRL system which is only observed at low RNA concentrations (8, 34).

The HCVp24 mRNAs were included in this assay as a negative control against nonspecific effects of polyadenylation on IRES-driven translation, since HCV genomic RNA is not polyadenylated but instead carries a conserved pyrimidine-rich X region at its 3′ end (20, 50). Not surprisingly, no significant stimulation of HCVp24 RNA translation was observed upon polyadenylation at any of the salt concentrations tested (Fig. 3D). As a further test against nonspecificity of the poly(A) effects on picornaviral IRES-driven translation, the various IRESp24 RNAs were also translated in standard RRL at the concentrations of added KCl or $MgCl_2$ which allowed significant poly(A) stimulation for each IRES in the depleted system (Table 1). With the exception of the HAV IRES, no significant stimulation of IRES-driven translation could be evidenced in the standard RRL system, indicating that poly(A) is important for picornavirus IRES-driven translation specifically in conditions under which cap-poly(A) synergy is observed on classical cellular mRNAs (Fig. 2; see also references 8 and 34).

We next determined whether polyadenylation was significantly altering the stability of the different IRES-containing mRNAs in the depleted system. Thus, the kinetics of protein synthesis on the poly(A)$^+$ and poly(A)$^-$ derivatives of a given IRES-p24 mRNA were evaluated in depleted RRL, in order to measure the functional stability of the different mRNAs (i.e., the stability of the actively translated fraction of programming mRNA). Figure 4A depicts the results of such an experiment with mRNAs carrying the HAV IRES, which in conditions of

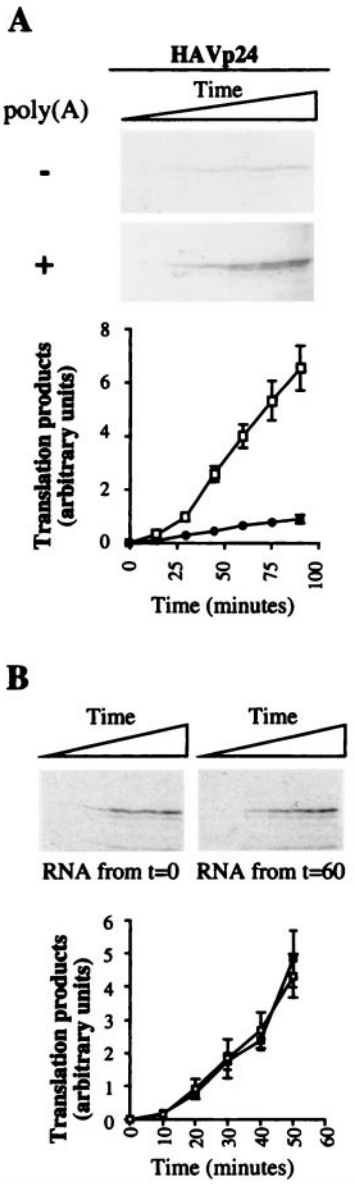


FIG. 4. Time course of protein synthesis from the pHAVp24-derived mRNAs in ribosome-depleted RRL. (A) Ribosome-depleted RRL reactions containing, respectively, 72 and 0.5 mM of added KCl and $MgCl_2$ were programmed with poly(A)$^-$ (filled circles) or poly(A)$^+$ (open squares) HAVp24 mRNAs at a 10-μg/ml final RNA concentration. Aliquots were removed at 15-min intervals from 0 to 90 min, and the translation products were analyzed as described in the legend to Fig. 2. (B) Polyadenylated HAVp24 mRNA was extracted from ribosome-depleted RRL translation reactions after 0 min (RNA from $t = 0$; open squares) and 60 min (RNA from $t = 60$; filled squares), as described in Materials and Methods, and quantified and used to reprogram ribosome-depleted RRL reactions as described for panel A, except that the final mRNA concentrations were 7.5 μg/ml. Aliquots were removed at 10-min intervals from 0 to 50 min, and the translation products were analyzed as described in the legend to Fig. 2. The error bars represent the standard deviation calculated from two independent experiments.

optimal salt was the most stimulated of the picornaviral elements upon polyadenylation. The kinetics of protein synthesis were linear for both the poly(A)$^-$ and poly(A)$^+$ forms of HAVp24 from 25 to 90 min of incubation. Similarly, the kinetics of protein synthesis were linear for both forms of mRNAs carrying the EMCV and PV IRESes (data not shown), indicating that the observed positive effects of poly(A) on translation did not stem from significant differences in mRNA functional stability. However, in the case of poly(A)$^+$ HAV RNA translation, a lag was observed in the appearance of translation products (Fig. 4A). Thus, it could conceivably be argued that this RNA was in some way processed before translation could begin. To examine this possibility, poly(A)$^+$ HAVp24 RNA reextracted from translation reactions after different times of incubation, was used to program fresh translation reactions. RNA extracted after 0 and 60 min of incubation showed identical translation kinetics (Fig. 4B), with a similar delay in the appearance of translation products to that observed in the original experiment (compare Fig. 4A and B), suggesting that poly(A)$^+$ HAV RNA had not been irreversibly processed after 60 min of translation in ribosome-depleted RRL. While we have no concrete explanation for this apparent lag, it is possible that the observed delay represents the time required to assemble initiation complexes on the particularly inefficient HAV IRES. Interestingly, a similar phenomenon has recently been reported for translation driven by the HAV IRES in synergistic HeLa cell extracts (1).

**The HCV 3′ X region is a nonspecific stimulator of translation.** Translation of mRNAs carrying the HCV IRES in depleted RRL was very efficient, irrespective of the poly(A) status and salt concentrations tested (see Fig. 3D). However, it was recently reported that HCV IRES-driven translation could be stimulated in vitro by the authentic HCV genomic 3′ X region (20, 21). Thus, additional cDNAs were constructed, based on p0p24 (as a control against nonspecific effects of X) or carrying the HCV IRES, in which the poly(A) tail was replaced by the 98-nt X region from HCV genotype 1b (Fig. 1). These cDNAs were transcribed in vitro in either capped and uncapped forms (for the p0p24 constructs) or only in an uncapped form (for pHCVp24 constructs), and the corresponding mRNAs were translated in the depleted RRL system at a variety of final RNA concentrations and in physiological salt concentrations (Fig. 5).

Translation driven by the HCV IRES was stimulated approximately threefold by the X region *in cis*, in agreement with previous studies in standard RRL (20). However, the X region in our system also significantly stimulated (3- to 4-fold) translation of uncapped 0p24 control mRNA, and moderately stimulated (1.5- to 3-fold) capped 0p24 mRNA translation, in contrast to previous reports which suggested that X-mediated stimulation was specific to IRES-driven translation. While we have no definitive explanation for this discrepancy, it should be noted that the HCV and 0p24 mRNAs tested here were translated under identical salt conditions (130 mM KCl and 0.9 mM $MgCl_2$). In contrast, while the IRES-carrying mRNAs were translated at 120 mM KCl by Ito et al. (20), the control cellular mRNAs were translated at 70 mM added KCl, conditions in which even cap dependency was minimal. In our experimental conditions, kinetics studies failed to detect any significant differences in functional mRNA stability between mRNAs with

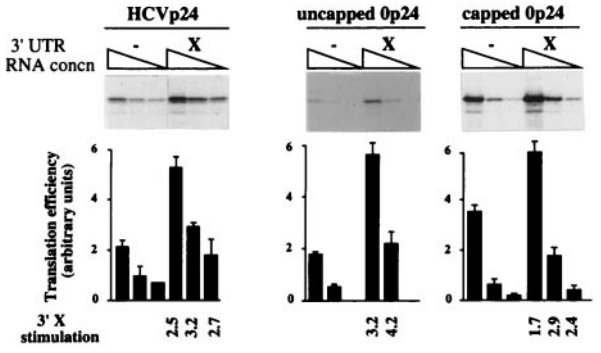


FIG. 5. Effect of the HCV 3′ X region on translation of capped, uncapped, or HCV IRES-containing mRNAs in ribosome-depleted RRL. Translation reactions were programmed with 10, 5, and 2.5 μg of uncapped pHCVp24-derived mRNAs per ml or 6.3, 3.1, and 1.6 μg of p0p24-derived mRNAs per ml with or without a cap and 3′ X region as indicated (+ or − cap/− or X). The final concentrations of KCl and $MgCl_2$ were, respectively, 130 and 0.9 mM. Translation products were analyzed as described in the legend to Fig. 2. Translation efficiencies and the 3′ X stimulation (calculated as translation efficiency with 3′ X divided by translation efficiency without 3′ X) are indicated for each lane in which translation products were easily detectable. The uncapped 0p24 panel was exposed four times longer than the HCVp24 and capped 0p24 panels. The error bars represent the standard deviation calculated from two independent experiments.

or without the X region, strongly suggesting that the nonspecific effects of X are not due to its ability to stabilize mRNAs in the depleted RRL system (data not shown). Further studies will be required to dissect the exact mechanism of X-mediated translation stimulation (see below).

**Poly(A)-mediated stimulation of picornaviral IRES-driven translation is sensitive to the disruption of the eIF4G-PABP interaction.** We previously demonstrated using the depleted RRL system that cap-poly(A) synergy on cellular mRNAs requires the eIF4G-PABP interaction (34). In effect, synergy was sensitive to the rotavirus NSP3 protein which has been shown to bind the N-terminal part of eIF4G and to displace PABP from the eIF4F complex (8, 34, 41). Since picornavirus IRES activity is clearly influenced by polyadenylation, we examined the effects of the NSP3 protein on poly(A)-mediated stimulation of translation of the different IRESp24 mRNAs. Toward this end, ribosome-depleted RRL translation reactions were preincubated with buffer or 10 μg of recombinant NSP3 fragment per ml (final concentration) and then programmed with various IRESp24 or 0p24 mRNAs (Fig. 6A). We have previously shown that this concentration of NSP3 induces maximal displacement of PABP from eIF4G when added to RRL (8, 34; data not shown). Indeed, this concentration of recombinant protein was sufficient to abolish cap-poly(A) synergy on a classical cellular mRNA in the depleted RRL system and to specifically reduce the translation efficiency of poly(A)$^+$ 0p24 mRNA to approach that of its poly(A)$^-$ counterpart (Fig. 6B). Conversely, NSP3 had no effect on the translation efficiency of poly(A)$^-$ or poly(A)$^+$ versions of HCV IRES-carrying mRNAs and, more interestingly, had no significant inhibitory effect on the stimulation of HCV IRES-driven translation afforded by the 3′ X region (Fig. 6C). Importantly, NSP3 dramatically reduced the poly(A)-mediated stimulation of PV, HAV, and EMCV IRES-driven translation (Fig. 6A). Thus, as

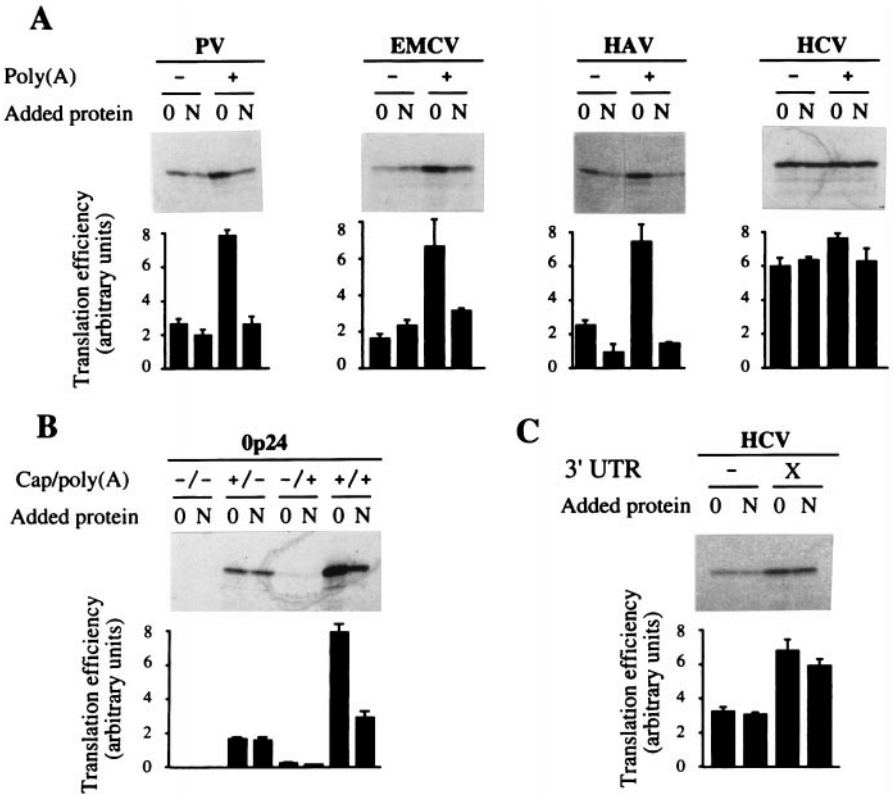


FIG. 6. Poly(A)-mediated stimulation of picornaviral IRES-driven translation requires the eIF4G-PABP interaction. Ribosome-depleted RRL was programmed with the indicated forms of the different IRESp24 mRNAs (A and C; final concentration, 10 μg/ml) or p0p24-derived mRNAs (B; final concentration, 6.3 μg/ml). Reactions contained salt concentrations, allowing comparable (three- to fourfold) stimulations upon polyadenylation of each IRES-p24 mRNA and easy detection of translation products (130 and 0.9 mM, respectively, of added KCl and $MgCl_2$ [0p24, EMCVp24, and HCVp24]; 119 mM KCl and 0.7 mM $MgCl_2$ [PVp24]; 72 mM KCl and 0.5 mM $MgCl_2$ [HAVp24]). Reactions were supplemented with H100 buffer (0 lanes) or recombinant truncated NSP3 protein (10 μg/ml; N lanes) in H100 buffer. Reactions programmed with PVp24 contained 2.5% (vol/vol) nuclease-treated HeLa cell S10 extract. Translation products were analyzed as described in the legend to Fig. 2. The error bars represent the standard deviation calculated from two or three independent experiments.

is the case for cellular mRNAs, the eIF4G-PABP interaction is indispensable for the poly(A) stimulation of picornaviral IRES-driven translation. It should also be noted that NSP3 reproducibly reduced translation efficiency of the poly(A)$^-$ form of mRNAs carrying the type I PV and especially the type III HAV IRESes [Fig. 6A, compare 0 and N lanes for each poly(A)-mRNA]. These effects are unlikely to result from a nonspecific inhibitory activity of NSP3 on translation, given the insensitivity of the HCV IRES and EMCVp24 poly(A)$^-$ mRNA translation to this protein. Instead, we believe that this inhibition reflects the sensitivity of the HAV IRES to the conformation of eIF4F, which is possibly altered by displacement of PABP and binding of NSP3 (Borman et al., submitted).

**Effects of NSP3 and 2A on poly(A)-mediated stimulation of IRES-driven translation.** The fact that the poly(A) mediated stimulation of type I PV IRES-driven translation requires the integrity of the eIF4G-PABP interaction raises important questions concerning the pertinence of poly(A)-mediated stimulation during the polioviral infectious cycle, since both PABP and eIF4G are cleaved by the PV 2A proteinase in the infected cell (25, 27). Thus, we examined the efficiency of IRES-driven translation in ribosome-depleted RRL which had been preincubated with either the NSP3 protein, the human rhinovirus 2A proteinase, or both NSP3 and 2A together (Fig. 7). The concentration of 2A proteinase used was sufficient to cleave all eIF4G in the depleted RRL extract (Fig. 7D, left panel). In contrast, although this 2A proteinase, like its PV counterpart, can cleave PABP upon prolonged incubation at 37°C (Borman et al., submitted) no such cleavage was evidenced under the conditions of our translation assays (Fig. 7D, right panel).

Inclusion of 2A proteinase in depleted RRL reactions significantly stimulated poly(A)$^-$ PVp24 mRNA translation [ca. 2.5-fold stimulation; Fig. 7A, compare lanes 0 and P, poly(A)$^-$], as described previously (2, 6, 53). This stimulation was insensitive to inclusion of recombinant NSP3 in the reactions [compare lanes 0, P, and NP, poly(A)$^-$]. A similar degree of stimulation (threefold) was afforded by polydenylation of the PVp24 mRNA in this particular experiment in depleted RRL [compare lanes 0 for poly(A)$^-$ and poly(A)$^+$], and this stimulation was abolished upon treatment with NSP3. However, the combination of 2A proteinase in translation reactions and a poly(A) tail at the PVp24 mRNA 3′ end did not result in an enhanced translation efficiency compared to that obtained with either poly(A) tail or 2A alone [Fig. 7A, compare lanes P and 0, poly(A)$^+$, and lane P, poly(A)$^-$, to lane 0, poly(A)$^-$]. Furthermore, poly(A)$^+$ PVp24 mRNA translation in the presence of 2A proteinase was resistant to NSP3 inhibition [Fig.

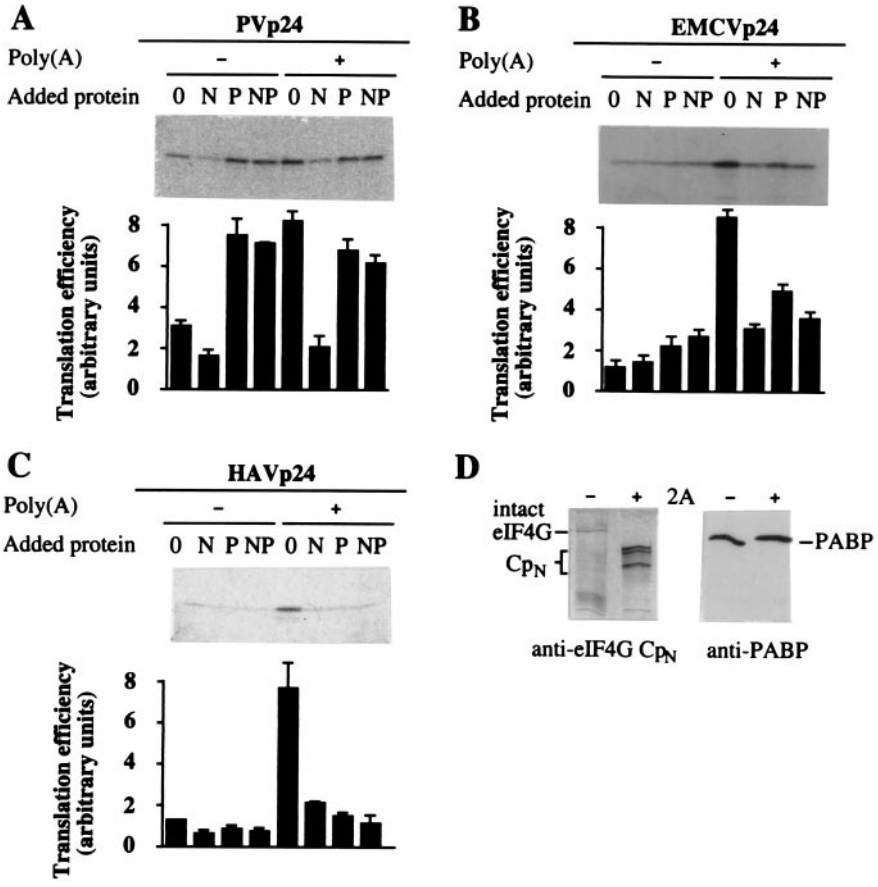


FIG. 7. Effects of NSP3 and HRV2 2A proteinase on poly(A)-mediated stimulation of picornavirus IRES-driven translation. (A to C) Ribosome-depleted RRL was programmed with 10 μg of the indicated forms of uncapped IRES-p24 mRNAs per ml and contained salt concentrations allowing comparable (ca. three- to fourfold) stimulations upon polyadenylation of each IRES-p24 mRNA and easy detection of translation products (130 and 0.9 mM, respectively, of added KCl and $MgCl_2$ [EMCVp24]; 119 mM KCl and 0.7 mM $MgCl_2$ [PVp24]; 72 mM KCl and 0.5 mM $MgCl_2$ [HAVp24]). Reactions programmed with PVp24 mRNAs also contained 2.5% (vol/vol) nuclease-treated HeLa cell S10 extract. Reactions were supplemented with H100 buffer (0 lanes), NSP3 protein (10 μg/ml; N lanes), rhinovirus 2A proteinase (40 μg/ml; P lanes) each in H100 buffer, or both NSP3 and 2A (10 and 40 μg/ml, respectively; NP lanes), also in H100 buffer. Translation products were analyzed as described in the legend to Fig. 2. The error bars represent the standard deviation calculated from two independent experiments. (D) Western blot analysis of eIF4G and PABP in 2A proteinase-treated depleted RRL translation extracts. Depleted RRL translation reactions were assembled as described in Materials and Methods with H100 buffer (− lanes) or 40 μg of of HRV2 2A proteinase per ml (final concentration) in H100 buffer (+ lanes), incubated at 30°C for 90 min, and then analyzed by Western blotting using antibodies raised against the N-terminal part of eIF4G ($Cp_N$) or against the C-terminal extremity of PABP as indicated. The positions of intact PABP, intact eIF4G, and the N-terminal cleavage product of eIF4G are indicated.

7A, compare lanes NP and N, poly(A)$^+$], indicating that, upon cleavage of eIF4G, polyadenylation no longer conferred an advantage on PV IRES-driven translation.

To examine whether this situation was specific to IRESes derived from viruses that cleave eIF4G, the same approach was carried out using EMCVp24 (Fig. 7B) or HAVp24 RNAs (Fig. 7C). For HAVp24 RNA, it could clearly be seen that cleavage of eIF4G inhibited rather than stimulated translation (Fig. 7C, compare lanes 0 and P) and that indeed the stimulation observed upon polyadenylation was abrogated by protease treatment of extracts [compare lanes 0 and P, poly(A)$^+$, with lane 0, poly(A)$^-$; Fig. 7C]. For EMCVp24 RNA translation, the situation was less clear-cut. Cleavage of eIF4G slightly stimulated (ca. 1.5-fold) poly(A)$^-$ EMCVp24 RNA translation [compare lanes 0 and P, poly(A)$^-$; Fig. 7B]. Conversely, protease treatment of extracts substantially reduced, but did not completely abolish, the stimulatory effects of polyadenylation [compare lanes 0 and P, poly(A)$^+$; Fig. 7B], a partial effect which remains difficult to explain clearly at present. Thus, cleavage of eIF4G significantly reduced the stimulatory effects of polyadenylation on translation driven by all of the picornaviral IRESes examined here but dramatically stimulated only PV IRES-driven translation.

## DISCUSSION

The classical closed-loop model for translation initiation on capped and polyadenylated cellular mRNAs dictates that efficiently translated mRNAs are noncovalently circularized via a cap-eIF4E-eIF4G-PABP-poly(A) tail interaction (13, 23, 43). Although picornaviral RNAs are polyadenylated, they are naturally uncapped and translated following IRES-driven internal

ribosome entry. Nevertheless, we previously showed that EMCV IRES-driven translation in a poly(A)-dependent RRL translation system was significantly stimulated upon polyadenylation of the RNA (34). This result was extended recently to include the PV and HAV IRESes by Bergamini et al. (1) in a poly(A)-dependent non-nucleased HeLa cell extract. Unfortunately, translation activity in these latter extracts was abolished by nuclease treatment. Thus, the presence of translationally active endogenous mRNAs precluded a dissection of the molecular mechanism of poly(A) stimulation of IRES-driven translation.

Here we have used our recently described poly(A)-dependent RRL extracts to address this question. Since poly(A) dependency in the RRL system results from partial depletion of ribosomes and their associated initiation factors to yield a competitive translational environment, the complication of the presence of heterologous mRNAs is circumvented (34). An additional advantage of the depleted RRL system is that translating mRNAs are extremely stable (8; this work), opening the possibility of analyzing uncapped IRES-carrying mRNAs without the need for nonphysiological 5′-end modification. Effectively, a limitation of the previously described HeLa cell extract (1) is that uncapped mRNAs were extremely unstable and had to be artificially capped with an ApppG cap analogue.

Picornavirus IRES-driven translation was stimulated by polyadenylation in the depleted RRL system. Under the optimal conditions for each IRES, the degree of stimulation ranged from approximately 3- to 4-fold (for EMCV) and 4- to 6-fold (for PV) to more than 10-fold (for HAV), results in good quantitative agreement with the results of Bergamini et al. (1), who observed 3-fold (for EMCV) and >10-fold stimulation indices with HAV and PV. It is possible that the more modest poly(A) stimulation of PV IRES-driven translation reported here stems from the necessity for PV IRES activity to include non-ribosome-depleted HeLa cell extract in the ribosome-depleted RRL system, which rendered the system less poly(A)-dependent as measured with control capped and/or polyadenylated mRNAs (Fig. 2; see also reference 8). The effects of polyadenylation on picornavirus IRES-driven translation reported here were specific, in that they were not transposable to the unrelated flaviviral HCV IRES (HCV viral RNA is not naturally polyadenylated) and did not result from any detectable differences in functional mRNA stability. It should also be noted that the different picornaviral IRESes are physiologically active in driving internal ribosome entry in the depleted RRL system. First, translation driven by the different uncapped, polyadenylated IRESes was some 20 to 40 times more efficient than an uncapped, polyadenylated control without an IRES (see, for example, Fig. 6). Second, the different IRESes were still functional when placed as the intercistronic spacer of a dicistronic mRNA (data not shown). Third, mutations in the PV IRES known to attenuate poliovirus vaccine strains were still deleterious for translation in the depleted RRL system (C. E. Malnou and K. M. Kean, unpublished data).

Importantly, poly(A)-mediated stimulation of picornaviral IRES-driven translation was sensitive to $MgCl_2$ and KCl concentrations and increased as near-physiological salt concentrations were attained, as we had previously shown for cap-poly(A) synergy on cellular mRNAs translated in this system (8). In addition, the salt optima of the various IRES types differed significantly. While this finding in itself is not necessarily surprising (see, for example, reference 2), important differences should be noted between the optima measured in standard RRL using nonpolyadenylated RNAs and those presented here with poly(A)$^+$ RNAs. The first concerns translation driven from the PV IRES which had been found to be extremely intolerant of $MgCl_2$ in standard RRL, a finding which was difficult to encompass within the context of the infected cell. In the depleted RRL system, translation driven from this element tolerates relatively high concentrations of $MgCl_2$. The second difference concerns the HAV IRES, for which discrepancies had previously been observed between efficient activity under most salt concentrations in standard RRL (2) and virtual inactivity in the intact cell (7). The current study shows that the HAV IRES appears poorly capable of driving translation in extracts in which ribosomes and/or initiation factors are limiting and in which salt concentrations are near physiological. Thus, with respect to both the PV and the HAV IRESes, translation of polyadenylated RNAs in the depleted RRL system appears to more closely reproduce the physiological situation than does translation of nonpolyadenylated RNAs in the standard, nondepleted RRL system.

As mentioned above, the novelty of the depleted RRL system, compared to the other poly(A)-dependent cell extracts described to date, is the absence of intact, endogenous competitor mRNAs. This makes it particularly appropriate for the dissection of the molecular mechanisms underlying poly(A)-mediated translation stimulation. In effect, in extracts which rely on mRNA competition to induce poly(A) dependency, any alterations of components of the translation machinery targeted to affect such poly(A) dependency cannot distinguish between the experimental and competitor RNAs. Thus, one cannot separate global nonspecific reduction of translation efficiency from specific effects on poly(A) dependency. In contrast, in the depleted RRL system, specific effects on poly(A) dependency are easily discerned (see, for example, Fig. 6). Thus, we employed the rotavirus NSP3 protein which interacts with eIF4G and evicts PABP from eIF4F to analyze the role of the eIF4G-PABP interaction in poly(A)-mediated stimulation of picornaviral IRES-driven translation. Poly(A) stimulation of translation driven by all three types of picornavirus IRES was abolished by recombinant NSP3, demonstrating that the integrity of the eIF4G-PABP interaction is required for this effect of poly(A). Thus, the mechanism of mRNA 5′- to 3′-end cross talk is functionally conserved between capped-polyadenylated and picornavirus IRES-carrying-polyadenylated mRNAs. However, one cannot invoke an eIF4E-cap interaction in the latter case. Rather, it is tempting to speculate that picornaviral mRNAs are circularized for translation via an IRES-eIF4G-PABP-poly(A) interaction at least early after infection (see Fig. 8), and we are currently evaluating this hypothesis directly. Indeed, the intact eIF4G molecule or a proteolytic C-terminal cleavage product of eIF4G has been shown to bind an internal region(s) of the different picornaviral IRESes (33, 39; Borman et al., submitted; for a review, see reference 26).

An important aspect of the results presented here concerns the effects of the human rhinovirus 2A proteinase, which cleaves eIF4G, on poly(A) stimulation of PV IRES activity. Translation driven by the PV IRES could be stimulated independently by either 2A proteinase or poly(A), in a nonadditive

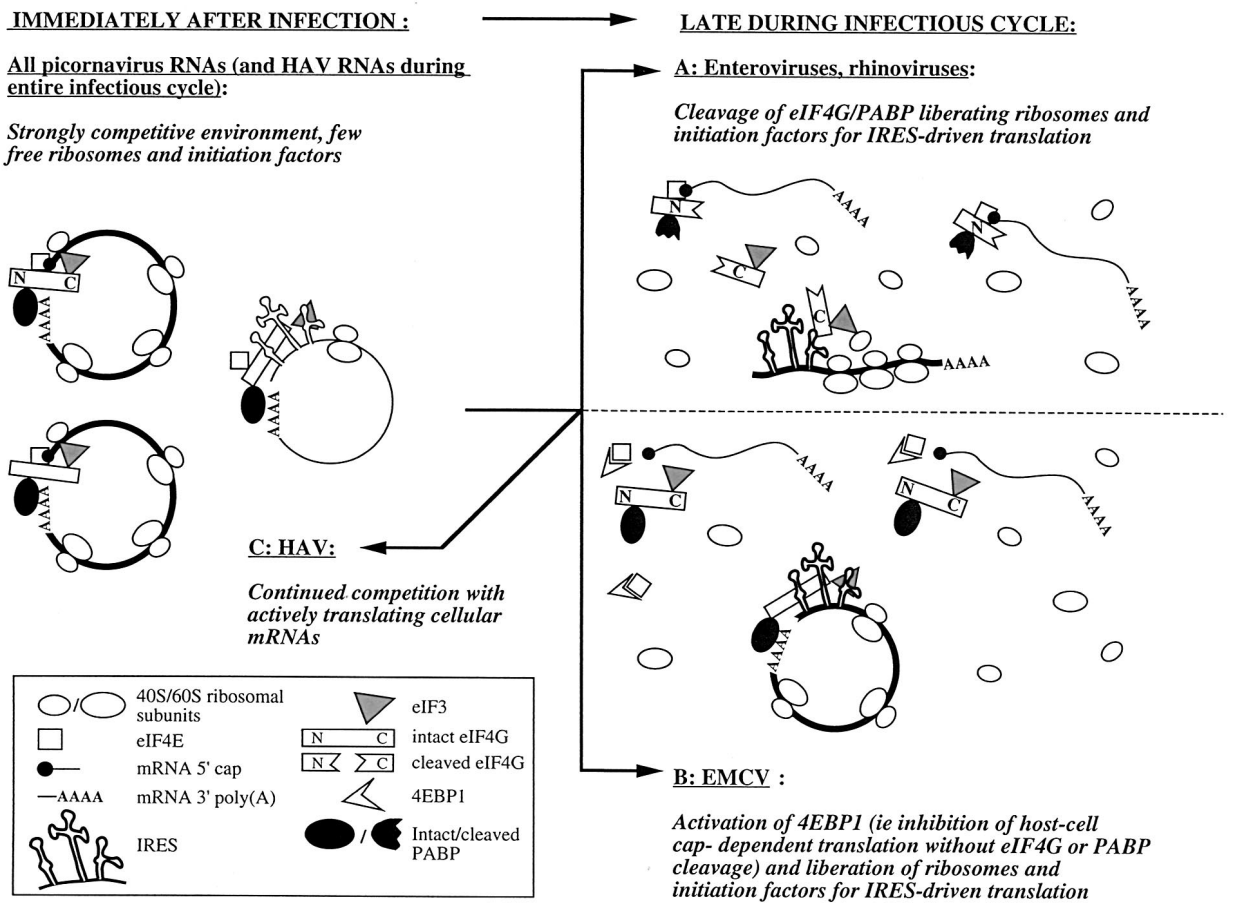


FIG. 8. Models depicting the circularization and translatability of cellular and viral mRNAs during the infectious cycle of different picornaviruses. In each panel the majority of the translation machinery is tied up by the mRNAs depicted as thick lines. Immediately after infection (see left side), we propose that the RNAs of all picornaviruses are circularized via the eIF4G-PABP interaction and probably require this interaction to compete with the actively translating circularized capped-polyadenylated cellular mRNAs. The entero- and rhinoviruses induce a dramatic inhibition of host cell protein synthesis, primarily via viral proteinase-mediated cleavage first of eIF4G and later of PABP, which will both block eukaryotic mRNA circularization. From the data presented here, it is clear that viral 5′- to 3′-end cross talk via the eIF4G-PABP interaction will be abolished concomitantly with host cell shutoff, when the host cell translation machinery is liberated for viral translation. However, continued circularization of viral RNAs via eIF4G-PABP is presumably rendered unnecessary since the corresponding IRESes can preferentially function with only the C-terminal cleavage product of eIF4G (right side, panel A). The efficient inhibition of host cell translation observed upon infection with EMCV results, at least in part, from the activation of eIF4E binding protein 1 (4EBP1) by its dephosphorylation (42a). Active (underphosphorylated) 4EBP1 has previously been shown to inhibit the interaction between eIF4E and eIF4G (17, 42a). Thus, once again, shutoff correlates with abrogation of cellular mRNA circularization. Since EMCV IRES activity does not require eIF4E (39), its translation will continue unabated. For this virus, which does not effectuate the cleavage of eIF4G or PABP, it seems reasonable to postulate that circularized viral genomes could persist throughout the infectious cycle (right side, panel B). Similarly, it seems likely that circularized viral RNAs will persist throughout HAV infection. However, since little or no inhibition of host cell protein sysnthesis is induced by HAV, one can predict that the circularized HAV RNAs will have to continue to compete for the translational machinery with circularized, efficiently translated host cell mRNAs throught the whole infectious cycle (left side, panel C). This may help to explain the extremely inefficient nature of HAV infection compared with the other picornaviruses.

manner. In effect, when PV IRES RNAs were translated in the presence of 2A proteinase, no additional stimulation was achievable upon polyadenylation. Most interestingly, translation of poly(A) plus PVp24 RNA was then resistant to NSP3. Thus, since the 2A proteinase did not cleave PABP under our reaction conditions, one can conclude that poly(A) stimulation is abolished upon cleavage of eIF4G. As host cell eIF4G is cleaved early in the PV infectious cycle (25), the results presented here strongly suggest that poly(A)-mediated circularisation of entero- and rhinovirus mRNA is important only for the first rounds of translation in the highly competitive cellular environment, before the shutoff of host cell translation. This mode of translation initiation would then be jettisoned in favor of IRES-driven translation mediated by the C-terminal cleavage product of eIF4G, which does not include the PABP interaction domain (6) (Fig. 8). Conversely, since eIF4G is not cleaved by HAV or EMCV, one can suggest that the corresponding viral genomes might remain in a circular form for translation throughout infection, with or without interruption of cellular mRNA circularization depending on the particular virus (Fig. 8).

Of the IRESes tested here, the HCV element was unique in

being stimulated by a 3′-end sequence in a PABP-eIF4G-independent manner. Although translation stimulation affected by the authenthic viral 3′ X region appeared not to be specific to the HCV IRES, it was totally resistant to NSP3. In fact, Ito and Lai suggested that HCV RNAs could be circularized by simultaneous binding of PTB to the HCV IRES and 3′ X region (21). Further studies will be necessary to test this hypothesis.

Finally, the apparent conservation of 5′- to 3′-end cross talk between capped and polyadenylated cellular mRNAs and picornaviral RNAs is likely to be particularly pertinent to the mechanism of translation of nonclassical cellular mRNAs. In effect, recent estimations suggested that as many as 10% of polyadenylated cellular mRNA species might possess IRESes. Several such cellular IRESes have been shown to be activated in vivo during stress or apoptosis (see, for example, reference 47), conditions in which eIF4G undergoes specific, limited proteolysis in a manner similar to that observed upon picornavirus infection (10). It remains to be determined whether such cellular IRES-carrying mRNAs can be encompassed within a closed-loop model of translation initiation. The translation systems described here should prove a very useful tool to address these questions.

## ACKNOWLEDGMENTS

We are grateful to Cécile Malnou and Sylvie van der Werf for their interest in this work and to Richard Paul for critical reading of the manuscript. We thank Didier Poncet and Nathalie Castagné for the gift of purified rotavirus NSP3 protein, Tim Skern for purified recombinant 2A proteinase, Bob Rhoads for antibodies raised against eIF4G, and M. Görlach for antibodies against PABP. We also thank Matthias Hentze and Encarna Martinez-Salas for communicating unpublished results.

This work was funded in part by a grant from the MRENT (réseau HCV). We also acknowledge support from the Programme de Recherche Clinique de l'Institut Pasteur, from a Contrat d'Incitation à la Recherche en vue d'Applications (CCV 8) from the Pasteur Institute, from the Association Française contre les Myopathies (AFM), and from the Agence Nationale de Recherches sur le SIDA (ANRS). Y.M.M. is supported by a doctoral fellowship from the Association pour la Recherche sur le Cancer (ARC).

## REFERENCES

1 **Bergamini, G., T. Preiss, and M. W. Hentze.** 2000. Picornavirus IRESes and the poly(A) tail jointly promote cap-independent translation in a mammalian cell-free system. RNA **6:**1773–1780.
2. **Borman, A. M., J.-L. Bailly, M. Girard, and K. M. Kean.** 1995. Picornavirus internal ribosome entry segments: comparison of translation efficiency and the requirements for optimal internal initiation *in vitro*. Nucleic Acids Res. **23:**3656–3663.
3. **Borman, A. M., F. G. Deliat, and K. M. Kean.** 1994. Sequences within the poliovirus internal ribosome entry segment control viral RNA replication. EMBO J. **13:**3149–3157.
4. **Borman, A., and R. J. Jackson.** 1992. Initiation of translation of human rhinovirus RNA: mapping the internal ribosome entry site. Virology **188:** 685–696.
5. **Borman, A. M., and K. M. Kean.** 1997. Intact eukaryotic initiation factor 4G is required for hepatitis A virus internal initiation of translation. Virology **237:**129–136.
6. **Borman, A. M., R. Kirchweger, E. Ziegler, R. E. Rhoads, T. Skern, and K. M. Kean.** 1997. eIF4G and its proteolytic cleavage products: Effect on initiation of protein synthesis from capped, uncapped and IRES-containing mRNAs. RNA **3:**186–196.
7. **Borman, A. M., P. Le Mercier, M. Girard, and K. M. Kean.** 1997. Comparison of picornaviral IRES-driven internal initiation of translation in cultured cells of different origins. Nucleic Acids Res. **25:**925–932.
8. **Borman, A. M., Y. M. Michel, and K. M. Kean.** 2000. Biochemical characterisation of cap-poly(A) synergy in rabbit reticulocyte lysates: the eIF4G-PABP interaction increases the functional affinity of eIF4E for the capped mRNA 5′ end. Nucleic Acids Res. **28:**4068–4075.
9. **Carter, M. S., K. M. Kuhn, and P. Sarnow.** 2000. Cellular internal ribosome entry site elements and the use of cDNA microarrays in their investigation, p. 615–635. *In* J. W. B. Hershey, M. B. Mathews, and N. Sonenberg (ed.), Translational control of gene expression. Cold Spring Harbor Laboratory Press, Cold Spring Harbor, N.Y.
10. **Clemens, M. J., M. Bushell, and S. J. Morley.** 1998. Degradation of eukaryotic polypeptide chain initiation factor (eIF) 4G in response to induction of apoptosis in human lymphoma cell lines. Oncogene **17:**2921–2931.
11. **Dasso, M. C., and R. J. Jackson.** 1989. Efficient initiation of mammalian mRNA translation at a CUG codon. Nucleic Acids Res. **17:**6485–6497.
12. **Gallie, D. R.** 1991. The cap and poly(A) tail function synergistically to regulate mRNA translational efficiency. Genes Dev. **5:**2108–2116.
13. **Gallie, D. R.** 1998. A tale of two termini: a functional interaction between the termini of an mRNA is a prerequisite for efficient translation initiation. Gene **216:**1–11.
14. **Gingras, A.-C., B. Raught, and N. Sonenberg.** 1999. eIF4 initiation factors: effectors of mRNA recruitment to ribosomes and regulators of translation. Annu. Rev. Biochem. **68:**913–963.
15. **Goldstein, N. O., I. U. Pardoe, and A. T. Burness.** 1976. Requirement of an adenylic acid-rich segment for the infectivity of encephalomyocarditis virus RNA. J. Gen. Virol. **31:**271–276.
16. **Görlach, M., C. G. Burd, and G. Dreyfuss.** 1994. The mRNA poly(A)-binding protein: localization, abundance, and RNA-binding specificity. Exp. Cell Res. **211:**400–407.
17. **Hershey, J. W. B., and W. C. Merrick.** 2000. Pathway and mechanism of initiation of protein synthesis, p. 33–88. *In* J. W. B. Hershey, M. B. Mathews, and N. Sonenberg (ed.), Translational control of gene expression. Cold Spring Harbor Laboratory Press, Cold Spring Harbor, N.Y.
18. **Hruby, D. E., and W. K. Roberts.** 1977. Encephalomyocarditis virus RNA. II. Polyadenylic acid requirement for efficient translation. J. Virol. **23:**338–344.
19. **Imataka, H., A. Gradi, and N. Sonenberg.** 1998. A newly identified N-terminal amino acid sequence of human eIF4G binds poly(A)-binding protein and functions in poly(A)-dependent translation. EMBO J. **17:**7480–7489.
20. **Ito, T., S. M. Tahara, and M. C. Lai.** 1998. The 3′ untranslated region of hepatitis C virus enhances translation from an internal ribosomal entry site. J. Virol. **72:**8789–8796.
21. **Ito, T., and M. C. Lai.** 1999. An internal polypyrimidine tract binding protein site in the hepatitis C virus RNA attenuates translation which is relieved by the 3′ untranslated sequence. Virology **254:**288–296.
22. **Jackson, R. J., and A. Kaminski.** 1995. Internal initiation of translation in eukaryotes: the picornavirus paradigm and beyond. RNA **1:**985–1000.
23. **Jacobson, A.** 1996. Poly(A) metabolism and translation: the closed-loop model, p. 451–480. *In* J. W. B. Hershey, M. B. Mathews, and N. Sonenberg (ed.), Translational control. Cold Spring Harbor Laboratory Press, Cold Spring Harbor, N.Y.
24. **Jansen, R. W., J. E. Newbold, and S. M. Lemon.** 1988. Complete nucleotide sequence of a cell culture-adapted variant of hepatitis A virus: comparison with wild-type virus with restricted capacity for *in vitro* replication. Virology **163:**299–307.
25. **Joachims, M., P. C. Van Breugel, and R. E. Lloyd.** 1999. Cleavage of poly(A)-binding protein by enterovirus proteases concurrent with inhibition of translation in vitro. J. Virol. **73:**718–727.
26. **Kean, K. M., Y. M. Michel, and A. M. Borman.** 1999. Viral exceptions to 5′-end dependent initiation of translation: is there really a difference in the mechanism of ribosome recruitment to capped and IRES containing mRNAs. Curr. Top. Virol. **1:**191–201.
27. **Kerekatte, V., B. D. Keiper, C. Badorff, A. Cai, K. U. Knowlton, and R. E. Rhoads.** 1999. Cleavage of poly(A)-binding protein by coxsackievirus 2A protease in vitro and in vivo: another mechanism for host protein synthesis shutoff? J. Virol. **73:**709–717.
28. **Kirchweger, R., E. Ziegler, B. J. Lamphear, D. Waters, H. D. Liebig, W. Sommergruber, F. Sobrino, C. Hohenadl, D. Blaas, R. E. Rhoads, and T. Skern.** 1994. Foot-and-mouth disease virus leader proteinase: purification of the Lb form and determination of its cleavage site on eIF4G. J. Virol. **68:**5677–5684.
29. **Kozak, M.** 1999. Initiation of translation in prokaryotes and eukaryotes. Gene **234:**187–208.
30. **Lamphear, B. J., R. Kirchweger, T. Skern, and R. E. Rhoads.** 1995. Mapping of functional domains in eukaryotic protein synthesis initiation factor 4G (eIF4G) with picornaviral proteases. Implications for cap-dependent and cap-independent translational initiation. J. Biol. Chem. **270:**21975–21983.
31. **Le, H., R. L. Tanguay, M. L. Balasta, C. C. Wei, K. S. Browning, A. M. Metz, D. J. Goss, and D. R. Gallie.** 1997. Translation initiation factors eIF-iso4G and eIF-4B interact with the poly(A)-binding protein and increase its RNA binding activity. J. Biol. Chem. **272:**16247–16255.
32. **Liebig, H. D., E. Ziegler, R. Yan, K. Hartmuth, H. Klump, H. Kowalski, D. Blaas, W. Sommergruber, L. Frasel, B. Lamphear, R. E. Rhoads, E. Kuechler, and T. Skern.** 1993. Purification of two picornaviral 2A proteinases: interaction with eIF4 and influence on *in vitro* translation. Biochemistry **32:**7581–7588.

33. **Lopez de Quinto, S., and E. Martinez-Salas.** 2000. Interaction of the eIF4G initiation factor with the aphthovirus IRES is essential for internal translation initiation in vivo. RNA **6:**1380–1392.
34. **Michel, Y. M., D. Poncet, M. Piron, K. M. Kean, and A. M. Borman.** 2000. Cap-poly(A) synergy in mammalian cell-free extracts: investigation of the requirements for poly(A)-mediated stimulation of translation initiation. J. Biol. Chem. **275:**32268–32276.
35. **Morley, S. J., P. S. Curtis, and V. M. Pain.** 1997. Translation's mystery factor begins to yield its secrets. RNA **3:**1085–1104.
36. **Ohlmann, T., M. Rau, V. M. Pain, and S. J. Morley.** 1996. The C-terminal domain of eukaryotic protein synthesis initiation factor (eIF) 4G is sufficient to support cap-independent translation in the absence of eIF4E. EMBO J. **15:**1371–1382.
37. **Pestova, T. V., C. U. T. Hellen, and I. N. Shatsky.** 1996. Canonical eukaryotic initiation factors determine initiation of translation by internal ribosomal entry. Mol. Cell. Biol. **16:**6859–6869.
38. **Pestova, T. V., I. N. Shatsky, S. P. Fletcher, R. J. Jackson, and C. U. T. Hellen.** 1998. A prokaryotic-like mode of cytoplasmic eukaryotic ribosome binding to the initiation codon during internal translation initiation of hepatitis C and classical swine fever virus RNAs. Genes Dev. **12:**67–83.
39. **Pestova, T. V., I. N. Shatsky, and C. U. T. Hellen.** 1996. Functional dissection of eukaryotic initiation factor 4F: the 4A subunit and the central domain are sufficient to mediate internal entry of 43S preinitiation complexes. Mol. Cell. Biol. **16:**6870–6878.
40. **Piron, M., T. Delaunay, J. Grosclaude, and D. Poncet.** 1999. Identification of the RNA-binding, dimerization and eIF4GI-binding domains of rotavirus nonstructural protein NSP3. J. Virol. **73:**5411–5421.
41. **Piron, M., P. Vende, J. Cohen, and D. Poncet.** 1998. Rotavirus RNA-binding protein NSP3 interacts with eIF4GI and evicts the poly(A) binding protein from eIF4F. EMBO J. **17:**5811–5821.
42. **Preiss, T., and M. W. Hentze.** 1998. Dual function of the messenger RNA cap structure in poly(A)-tail-promoted translation in yeast. Nature **392:**516–520.
42a. **Raught, B., A.-C. Gingras, and N. Sonenberg.** 2000. Regulation of ribosomal recruitment in eukaryotes, p. 807–825. *In* J. W. B. Hershey, M. B. Mathews, and N. Sonenberg (ed.), Translational control of gene expression. Cold Spring Harbor Laboratory Press, Cold Spring Harbor, N.Y.
43. **Sachs, A. B., P. Sarnow, and M. W. Hentze.** 1997. Starting at the beginning, middle and end: translation initiation in eukaryotes. Cell **89:**831–838.
44. **Sarnow, P.** 1989. Role of 3′-end sequences in infectivity of poliovirus transcripts made in vitro. J. Virol. **63:**467–470.
45. **Schwartz, D. C., and R. Parker.** 2000. Interaction of mRNA translation and mRNA degradation in *Saccharomyces cerevisiae*, p. 807–825. *In* J. W. B. Hershey, M. B. Mathews, and N. Sonenberg (ed.), Translational control of gene expression. Cold Spring Harbor Laboratory Press, Cold Spring Harbor, N.Y.
46. **Spector, D. H., and D. Baltimore.** 1974. Requirement of 3′-terminal poly(adenylic acid) for the infectivity of poliovirus RNA. Proc. Natl. Acad. Sci. USA **71:**2983–2987.
47. **Stoneley, M., S. A. Chappell, C. L. Jopling, M. Dickens, M. MacFarlane, and A. E. Willis.** 2000. c-myc protein synthesis is initiated from the internal ribosome entry segment during apoptosis. Mol. Cell. Biol. **20:**1162–1169.
48. **Tarun, S. Z., Jr., and A. B. Sachs.** 1995. A common function for mRNA 5′ and 3′ ends in translation initiation in yeast. Genes Dev. **9:**2997–3007.
49. **Tarun, S. Z., Jr., and A. B. Sachs.** 1996. Association of the yeast poly(A) tail binding protein with translation initiation factor eIF-4G. EMBO J. **15:**7168–7177.
50. **Tsuchihara, K., T. Tanaka, M. Hijikata, S. Kuge, H. Toyoda, A. Nomoto, N. Yamamoto, and K. Shimotohno.** 1997. Specific interaction of polypyrimidine tract-binding protein with the extreme 3′-terminal structure of the hepatitis C virus genome, the 3′ X. J. Virol. **71:**6720–6726.
51. **Wells, S. E., P. E. Hillner, R. D. Vale, and A. B. Sachs.** 1998. Circularization of mRNA by eukaryotic translation initiation factors. Mol. Cell **2:**135–140.
52. **Yan, R., W. Rychlik, D. Etchison, and R. E. Rhoads.** 1992. Amino acid sequence of the human protein synthesis initiation factor eIF4G. J. Biol. Chem. **267:**23226–23231.
53. **Ziegler, E., A. M. Borman, F. G. Deliat, H.-D. Liebig, D. Jugovic, K. M. Kean, T. Skern, and E. Kuechler.** 1995. Picornavirus 2A proteinase-mediated stimulation of internal initiation is dependent on enzymatic activity and the cleavage products of cellular proteins. Virology **213:**549–557.